



Read-Green points and level crossings in XXZ central spin models and $p_x + ip_y$ topological superconductors

Alexandre Faribault, Houda Koussir , and Mohamed Houssein Mohamed
Université de Lorraine, CNRS, LPCT, F-54000 Nancy, France

 (Received 19 September 2019; published 21 November 2019)

In this work, we study the full set of eigenstates of a $p_x + ip_y$ topological superconductor coupled to a particle bath, which can be described in terms of an integrable Hamiltonian of the Richardson-Gaudin class. The results derived in this work also characterize the behavior of an anisotropic XXZ central spin model in an external magnetic field since both types of Hamiltonian are known to share the exact same conserved quantities, making them formally equivalent. We show how by ramping the coupling strength (or equivalently the magnetic field acting in the z -direction on the central spin), each individual eigenstate undergoes a sequence of gain/loss of excitations when crossing the specific values known as Read-Green points. These features are shown to be completely predictable for every one of the 2^N eigenstates, using only two integers easily obtainable from the zero-coupling configuration, which defines the eigenstate in question. These results provide a complete map of the particle-number sectors (superconductor) or magnetization sectors (central spin) involved in the large number of level crossings that occur in these systems at the Read-Green points. It further allows us to define quenching protocols that could create states with remarkably large excitation-number fluctuations.

DOI: [10.1103/PhysRevB.100.205420](https://doi.org/10.1103/PhysRevB.100.205420)

I. INTRODUCTION

Since its first explanation by Bardeen, Cooper, and Schrieffer in 1957 [1], the theoretical description of superconducting systems has been vastly enriched by going beyond their original mean-field treatment of s -wave pairing interactions. An exact solution to the reduced s -wave BCS pairing Hamiltonian was found by Richardson in 1963 [2,3], a result that saw an important surge in interest in the early 2000s [4,5] in the theoretical description of experiments on superconducting nanograins [6–8].

It was also around that time that the s -wave pairing model was explicitly shown, in 1997, to be integrable when Cambiaggio *et al.* [9] explicitly found the set of commuting conserved operators defining its quantum integrability. Using an Anderson pseudospin representation, this set of commuting operators then makes the s -wave pairing problem equivalent to an isotropic XXX Gaudin magnet [10–12].

These ideas have then been built upon to build integrable pairing Hamiltonians from anisotropic Richardson-Gaudin models [13–15]. Integrable BCS pairing models with $p_x + ip_y$ symmetry have then been studied beyond the common mean-field approximation using the massive simplifications that integrability and the Bethe ansatz solution can provide [16–20]. Such models attract a strong interest since they can exhibit topological superconductivity [21–23] whose occurrence could possibly be exploited in quantum computational applications [24–26].

A recent result, upon which this work builds, is the observation by Claeys *et al.* [27]. By coupling weakly such a $p + ip$ superconducting system to an external bath of particles, we break the $U(1)$ symmetry, which enforces the conservation of the number of Cooper pairs. In doing so, the ground state of the system, when raising the coupling constant g , will undergo

a series of steps by systematically gaining a single Cooper pair when the coupling goes through specific values $g = g_i$, dubbed Read-Green points. The resulting ground state at, and around, these points then becomes a coherent superposition of M and $M + 1$ Cooper pair states that exhibits pair number fluctuations. This is made possible by the weak coupling to the bath, which turns into avoided crossings, the level crossings between number-conserving sectors that would occur at these specific couplings in a closed (number-conserving) system.

In this work, a similar study is carried out for every eigenstate of the system in order to characterize the behavior of the full set of eigenstates across those Read-Green points. We first show explicitly that a steplike structure occurs over the (almost) complete Hilbert space and that it can be richer for the excited states than the one the ground state undergoes. Indeed, excited states can show both gains and losses of excitations when g goes across a Read-Green point, and these gains and losses can involve much more than a single excitation. Secondly, we demonstrate that the sequence of gains and losses can be completely predicted using only two, state-specific, integers, which are then sufficient to know the complete profile of excitation number that each individual eigenstate goes through as the coupling is varied. Finally, through this full understanding of the involved (avoided) crossings, we discuss a quenching protocol designed to create specific states, which should allow remarkably large number fluctuations by hybridizing two sectors at filling factors $\rho \approx 0$ and $\rho \approx 1$.

II. RICHARDSON-GAUDIN MODELS

The integrability of the $p + ip$ pairing models is fundamentally linked to the fact that they can be built as a linear

combination of the set of N mutually commuting operators given, in Anderson pseudospin representation, by

$$\tilde{R}_i = \frac{1}{g} \sigma_i^z + \sum_{j \neq i}^N [X_{ij} (\sigma_i^x \sigma_j^x + \sigma_i^y \sigma_j^y) + Z_{ij} \sigma_i^z \sigma_j^z]. \quad (1)$$

Here $i = 1, 2, \dots, N$ labels one of the possible momenta k_i at which one can either find a Cooper pair or not. To ensure the commutation rules $[R_i, R_j] = 0$ and consequently integrability, one needs to have X_{ij} and Z_{ij} parametrized as $X_{ij} = \frac{\sqrt{(\alpha\epsilon_i + \beta)(\alpha\epsilon_j + \beta)}}{\epsilon_i - \epsilon_j}$ and $Z_{ij} = \frac{\alpha\epsilon_j + \beta}{\epsilon_i - \epsilon_j}$ for arbitrary parameters α, β and $(\epsilon_1, \dots, \epsilon_N)$ [12,28,29].

Each of these individual conserved charges defines an anisotropic (XXZ) central spin model in which i now labels each of the N spins present. The operator \tilde{R}_i then corresponds to a Hamiltonian in which the central spin, of index i , feels a z -oriented magnetic field (chosen here as $B_z = \frac{1}{g}$) and is also anisotropically coupled to each of the other $N - 1$ individual spins. The fermionic $p + ip$ pairing Hamiltonian is obtained through a well-documented [13,16–20,27,30,31] sum over these conserved charges using the Cooper-pair realization of the SU(2) algebra, which makes $\sigma_i^z = c_{k_i}^\dagger c_{k_i} + c_{-k_i}^\dagger c_{-k_i} - 1$, while σ_i^\pm creates or annihilates a Cooper pair in the $(k_i, -k_i)$ momentum state. The parameter g , which defines an external magnetic field in the central spin models, now plays the role of the pairing strength. Since both the pairing and the central spin model are defined by the same set of commuting conserved operators, they share the same eigenbasis, which allows us to discuss the properties of the eigenstates of both models in the exact same terms. Throughout this work, we will therefore use the term “number of excitations” in order to describe either the total number of Cooper pairs in a pairing model or the total number of up-pointing spins in the central spin model.

The common eigenstates of the conserved charges (1), and therefore of the corresponding superconducting pairing model, are all such that they have a fixed total number of excitations since each of the \tilde{R}_i operators also commutes with the operator $\hat{M} = \frac{1}{2} \sum_{i=1}^N \sigma_i^z + 1$ whose eigenvalues $0, 1, 2, \dots, N$ define this total number. This conservation reflects an underlying U(1) symmetry. Adding an XY-plane component to the magnetic field or equivalently for the superconductor by coupling it to an external particle bath will break this symmetry. Remarkably, one can do so without breaking the integrability of the system [20,27,29,31,32] as, indeed, the following set of commuting operators:

$$R_i = \frac{\gamma}{\sqrt{\alpha\epsilon_i + \beta}} \sigma_i^x + \frac{\lambda}{\sqrt{\alpha\epsilon_i + \beta}} \sigma_i^y + \frac{1}{g} \sigma_i^z + \sum_{j \neq i}^N [X_{ij} (\sigma_i^x \sigma_j^x + \sigma_i^y \sigma_j^y) + Z_{ij} \sigma_i^z \sigma_j^z], \quad (2)$$

still commute with one another, therefore defining an integrable model allowing us to retain the major simplifications that integrability has to offer. Our numerical study of the model's eigenstates makes use of recent work [28,29,33], which has shown explicitly that the set of eigenvalues (r_1, r_2, \dots, r_N) [of the operators (R_1, R_2, \dots, R_N) given in Eq. (2)], which define each individual eigenstate, are also

given by the set of solutions of a simple system of N quadratic equations:

$$r_i^2 = \sum_{j \neq i} \Gamma_{ij} r_j + K_i, \quad (3)$$

with $\Gamma_{ij} = 2 \frac{\alpha\epsilon_j + \beta}{\epsilon_i - \epsilon_j}$ and $K_i = \frac{\gamma^2 + \lambda^2}{\alpha\epsilon_i + \beta} + \frac{1}{g^2} + \sum_{j \neq i}^N \left(\frac{2(\alpha\epsilon_i + \beta)(\alpha\epsilon_j + \beta) + (\alpha\epsilon_j + \beta)^2}{(\epsilon_i - \epsilon_j)^2} \right)$ [33]. The knowledge of the eigenvalues (r_1^n, \dots, r_N^n) associated with the eigenstate of index n , $|\psi_n\rangle$, in conjunction with the quadratic equation they obey, gives simple numerical access to the expectation values $\langle \psi_n | \sigma_i^\alpha | \psi_n \rangle$ of every local spin operator $i = 1, \dots, N$, in any direction $\alpha = x, y, z$, by direct use of the Hellmann-Feynman theorem [28].

At any given value of g , i.e., of the magnetic field or the coupling strength, each individual eigenstate can be uniquely indexed by specifying its $g = 0$ parent state. Indeed, each eigenstate at finite g can be built by deforming a given $g = 0$ eigenstate (parent state) by incrementing the coupling strength in small steps. The previously found eigenvalues $[r_1(g - \Delta g) \dots r_N(g - \Delta g)]$ provide an approximative solution for the eigenvalues at g that, for Δg small enough, stays within a particular solution's basin of attraction of an iterative Newton-Raphson algorithm. By labeling the spins in such a way that $\epsilon_1 < \epsilon_2 < \epsilon_3 < \dots < \epsilon_N$, we will use the notation \bullet for an up-spin and \circ for a down-spin so that, for example, the parent ($g = 0$) eigenstate $|\uparrow_1\rangle \otimes |\downarrow_2\rangle \otimes |\downarrow_3\rangle \otimes |\uparrow_4\rangle \otimes |\downarrow_5\rangle \dots \otimes |\uparrow_N\rangle$ will be represented as $\bullet \circ \circ \bullet \circ \dots \bullet$, with the symbols ordered from left to right in increasing ϵ_i order. In the central spin model described by the Hamiltonian R_1 , it means that σ_1 is considered the central spin while the environmental spins will be numbered in decreasing order of the magnitude of their coupling to the central spin, i.e., the closer a spin is to the central one, the larger is its coupling and therefore the lower is its index.

III. RESULTS

Using this g -scanning algorithm for the superconductor's ground state, it was shown by Claeys *et al.* [27] that, in the presence of weak coupling to a bath (superconductor) or an in-plane-magnetic field (central spin) ($\lambda, \gamma \neq 0$), the ground state gets deformed in such a way that it gains a single Cooper pair every time it goes through one of the specific values of the coupling g corresponding to the Read-Green points:

$$|g| = \frac{1}{N - 2M - 1} \quad \forall M = 0, 1, \dots, N/2, \quad (4)$$

at which $\frac{1}{|g|}$ corresponds to an integer in the series $1, 3, 5, \dots, N - 1$. This specific steplike behavior of the total number of excitations is shown in the upper left panel of Fig. 2 of this work, while the corresponding expectation values of the individual spins can be seen in panel (a) of Fig. 1. If we had $\lambda, \gamma = 0$, the resulting number-conserving system would show a true energy level crossing between the M and $M + 1$ excitation-number sectors, while here, at and around those Read-Green points, the ground state hybridizes between those two sectors of the Hilbert space.

Since the quadratic equations (3) give us simple access to the properties of individual eigenstates, the same study can

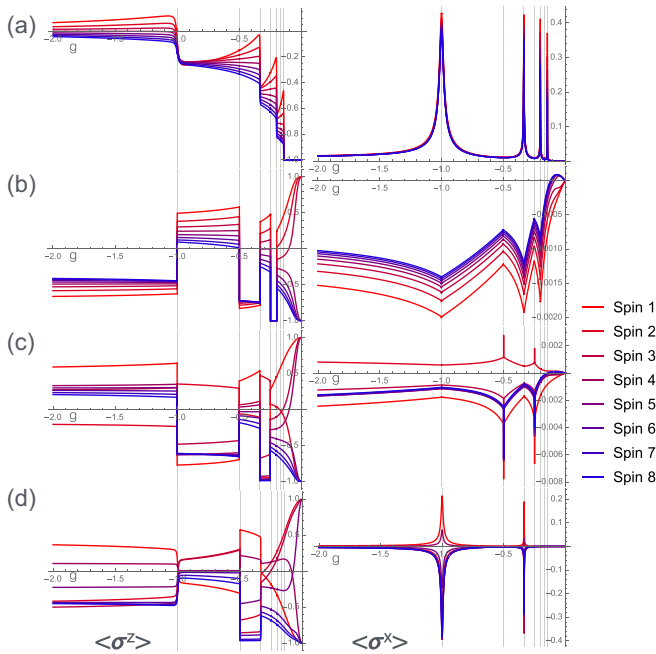


FIG. 1. Local expectation values $\langle \sigma_i^z \rangle$ and $\langle \sigma_i^x \rangle = \langle \sigma_i^y \rangle$ for $\epsilon_i = i$, $\gamma = \lambda = 0.005$, $\alpha = \beta = 1$ for a selection of eigenstates, from top to bottom: (a) $\circ \circ \circ \circ \circ \circ \circ \circ$, (b) $\bullet \bullet \bullet \circ \circ \circ \circ \circ$, (c) $\bullet \bullet \bullet \bullet \circ \circ \circ \circ$, and (d) $\circ \bullet \bullet \circ \bullet \circ \circ \circ$. The vertical lines mark the Read-Green points at $\frac{1}{|g|} = 7, 6, 5, 4, 3, 2, 1$.

be carried out, in a short amount of computation time, for every state in a small enough system. Here we choose to do so for the $2^N = 256$ states of a system of eight spins since it is sufficient to reach clear conclusions about the system's generic structure. Figure 1 presents the expectation values of σ_i^z and σ_i^x of four specific eigenstates as g is varied. The parameters of the model were chosen as $\epsilon_i = i$, $\alpha = \beta = 1$, and $\gamma = \lambda$ so that, by symmetry, σ_i^y behaves exactly as σ_i^x .

The ground state presented in panel (a) shows the behavior described previously: gaining a single excitation each time $\frac{1}{|g|}$ goes through odd integer values. As seen in [27], at these points a strong resonance in the in-plane magnetization $\langle \sigma_x \rangle$ is also found, indicating that individual spins are in a coherent superposition of their two σ_z eigenstates: $|\uparrow_i\rangle, |\downarrow_i\rangle$. However, from the other eigenstates presented, we immediately see that they too can undergo similar restructuring when going through those specific values of $\frac{1}{|g|}$. We first notice that for the excited states of the system, these can occur at every integer value $\frac{1}{|g|}$ between 1 and $N - 1$, whereas the ground state only gained an excitation at odd integer points. One also finds, by looking at the scale of the plots, that the resonant $\langle \sigma_x \rangle$ behavior is found, in the presented cases, only for the states of panels (a) and (d), while panels (b) and (c) only show extremely weak in-plane expectation values. This can be easily understood since the full classification presented below will allow us to understand that the eigenstate in panels (a) and (d) hybridizes between sectors containing M and $M + 1$ excitations while (b) and (c) involves two sectors that differ by more than one excitation, sectors between which σ_x has no matrix element connecting them.

To characterize these (avoided) crossings and the excitation-number sectors that they involve, one can now turn to the expectation value of the total excitation number operator: $\frac{1}{2} \sum_{i=1}^N \langle \sigma_i^z + 1 \rangle$. The behavior of every one of the 2^N eigenstates is presented in Fig. 2.

As one can readily see, a limited number of possible behaviors are exhibited. Indeed, for large subsets of eigenstates, the plots are indistinguishable from one another, undergoing the exact same sequence of gains and losses of excitations as they go through the Read-Green points. For the 256 states plotted, only 25 distinct behaviors are observed. Remarkably, each individual state's sequence of restructuring is entirely predictable by specifying only two integers defined by the structure of the $g = 0$ parent state, namely the number of excitations it contains, M_0 , and a second integer, r (defined in the next section), which can also be computed in a simple way.

IV. CLASSIFICATION OF THE PROFILES OF MAGNETIZATION/NUMBER OF PAIRS

As seen in Fig. 2, each $g = 0$ parent state defined by a given pair (M_0, r) will have the same structure as g is varied. Here, M_0 is simply the total number of up-spins (Cooper pairs) in the parent state, and the integer r can also be found directly by specifying the parent state's structure. It can be calculated by first separating the state into P contiguous blocks that contain only "down-spins" on the left and "up-spins" on the right. For example, a parent state given by

$$\circ \circ \bullet \bullet \bullet \circ \circ \bullet \bullet \bullet \bullet \bullet \circ \circ \circ$$

would be grouped into $P = 3$ blocks:

$$\boxed{\circ \circ \bullet \bullet \bullet} \boxed{\circ \circ \bullet} \boxed{\circ \circ \bullet \bullet \bullet \bullet} \circ \circ \circ$$

One then defines the excess number of "up-spins" in the rightmost block (numbered P) as $r_P = \max(N_{\bullet}^P - N_{\circ}^P, 0)$, with N_{\bullet}^P the number of up-spins and N_{\circ}^P the number of down-spins in block P . One then moves on to block $P - 1$ for which the number of spins up in excess is computed after carrying over the excess number from the preceding block so that $r_{P-1} = \max(N_{\bullet}^{P-1} + r_P - N_{\circ}^{P-1}, 0)$. The procedure is kept going by computing $r_{P-2} = \max(N_{\bullet}^{P-2} + r_{P-1} - N_{\circ}^{P-2}, 0)$ until the excess number from the last block gives us $r \equiv r_1 = \max(N_{\bullet}^1 + r_2 - N_{\circ}^1, 0)$. In the example above, the rightmost block $P = 3$ leads to $r_3 = 2$ (i.e., $4 \bullet - 2 \circ$). The two up-spins in excess are then added to the second block leading to $r_2 = 1$ [i.e., $1 \bullet + 2 \bullet$ (from the third block) $- 1 \circ$]. This excess spin is then added to the last block finally giving $r = 2$ [i.e., $3 \bullet + 1 \bullet$ (from the preceding block) $- 2 \circ$]. Interestingly, this specific integer r has also been shown to give, for a given $g = 0$ configuration, the number of Bethe roots that will diverge at large g for any eigenstate of the isotropic XXX Richardson-Gaudin model [34,35].

As we now show, the specific sequence underwent by any (M_0, r) state obeys relatively simple rules. As seen in Fig. 2, at the Read-Green points at which an (M_0, r) -state sees a loss of excitations, it will always correspond to a loss of exactly r excitations. Gains, on the other hand, always happen by gaining $r + 1$ excitations. Moreover, they are always in strict alternation such that, moving from $g = 0$, the state will, at a

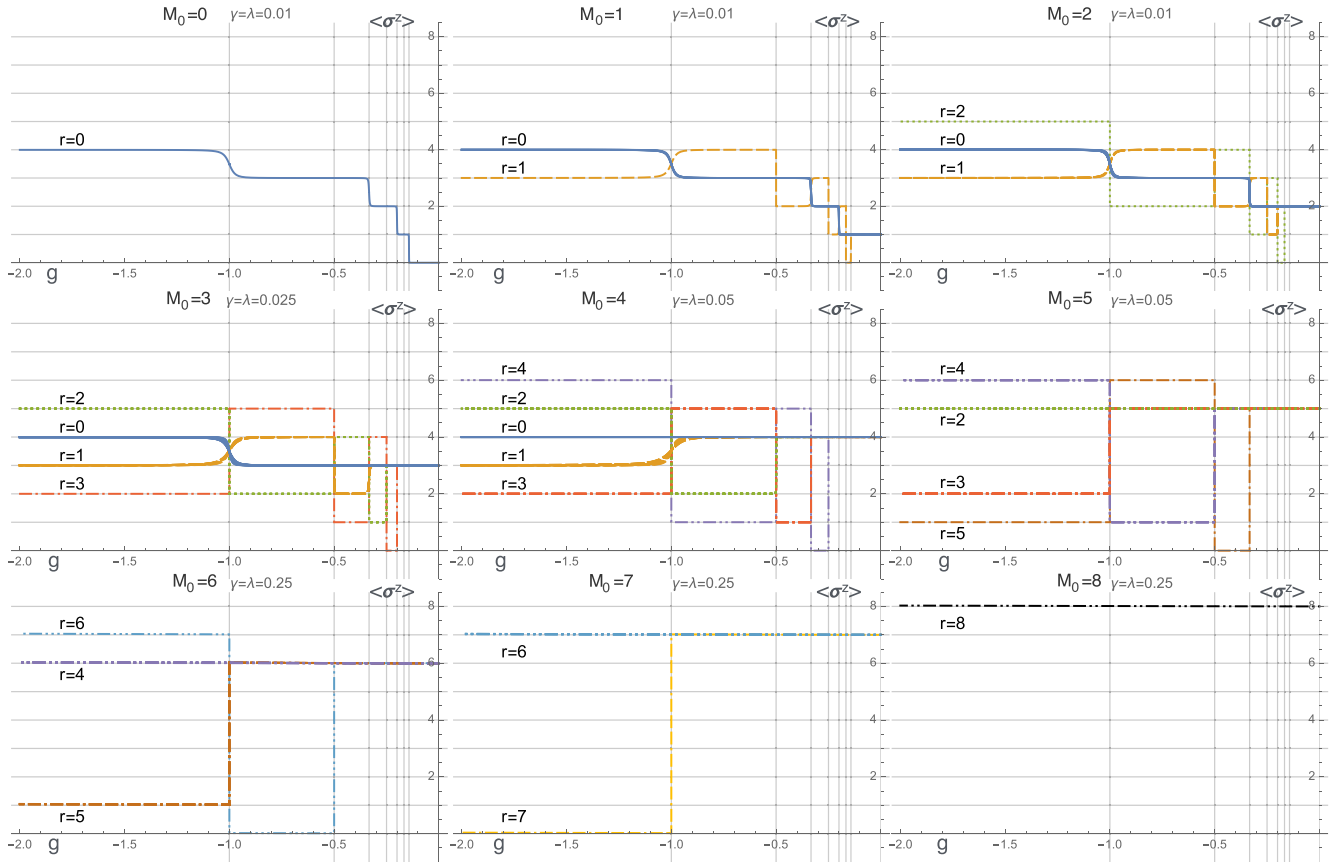


FIG. 2. z -axis magnetization of the 2^N eigenstates as a function of the parameter g . The $\frac{N!}{(N-M)!M_0!}$ eigenstates whose parent state at $g = 0$ has M_0 excitations are plotted in different panels. For a given M_0 , all states with a given integer r become (nearly) indistinguishable from one another.

specific Read-Green point $g_s(M_0, r)$, first undergo a loss of r excitation followed at the next Read-Green point by a gain of $r + 1$. This sequence will be repeated until the last point at $g = 1$ is reached. This statement is also true when $r = 0$, which can then be understood as a “loss of zero excitation” followed by a gain of one as was the case for the superconducting ground state, for example.

The last detail that remains to be specified is the specific Read-Green point $g_s(M_0, r)$ at which this “loss of r /gain of $r + 1$ ” sequence starts. It is simple to verify that for every case in which $r = M_0$, the loss/gain sequence begins specifically at the M_0 th Read-Green point (numbering them from 1 to $N - 1$ in order of their magnitude $|g|$). For a given M_0 value, one then sees that when r goes down by 1 (from M_0 to $M_0 - 1$ to $M_0 - 2$ and so on), the start of the sequence gets shifted to the next Read-Green point. All in all, for $g < 0$, any given eigenstate whose $g = 0$ parent state is defined by (M_0, r) will undergo an alternation of losses of r excitations followed by gains of $r + 1$ starting with a first loss at the $(2M_0 - r)$ th RG point:

$$g_s(M_0, r) = \frac{1}{N - 2M_0 + r}. \quad (5)$$

Starting at half-filling $M_0 = N/2$, the lowest possible value of r , namely $2M_0 - N$, would place $|g_s|$ beyond the last

Read-Green point, and this small subset of states are the only ones that never undergo any such restructuring, i.e., they never have any (avoided) crossings with states from a different sector. For clarity, the presented case, $N = 8$, is also detailed in Table I.

Each of these losses/gains corresponds, in the underlying number-conserving $U(1)$ -symmetric models, to a level crossing between two orthogonal sectors with a different number of excitations. These results, therefore, also provide a complete map of the magnetization/filling-factor sectors involved in the numerous degeneracies that occur at each of these Read-Green points in the excitation-number-conserving systems. Using the Bethe ansatz approach in the number-conserving case, it was demonstrated that at each Read-Green point there exists a duality that allows pairs of degenerate eigenstates to be created by adding, to the state in the lowest number sector, a given precise number of zero-energy excitations (Cooper pairs/up-pointing spins) [14, 16, 17]. The number of these zero-energy excitations defines a proper winding number, which characterizes the state’s topology. In the problem treated here, by lifting the requirement of number conservation, each individual eigenstate, when deformed through a Read-Green point, is no longer required to have those zero-energy pairs and to go through the corresponding change in its topology. Indeed, states now simply lose (or gain) the

TABLE I. The gains/losses are presented from left to right in order of increasing $|g|$, i.e., $g = (-\frac{1}{7}, -\frac{1}{6}, -\frac{1}{5}, -\frac{1}{4}, -\frac{1}{3}, -\frac{1}{2}, -1,)$. The point at which the sequence (loss $-r$ /gain $r + 1$) starts is underlined and bold. The grayed-out cells are those where no gain or loss of excitations occurs since the start of the sequence would put it at a value of g beyond the last Read-Green point $|g| = 1$. The white cells correspond to values of r that are impossible by construction.

$g < 0$	$M_0=0$	$M_0=1$	$M_0=2$	$M_0=3$	$M_0=4$	$M_0=5$	$M_0=6$	$M_0=7$	$M_0=8$
$r=0$	+1 -0 +1 -0 +1 -0 +1	0 -0 +1 -0 +1 -0 +1	0 0 0 -0 +1 -0 +1	0 0 0 0 0 -0 +1	No change	-	-	-	-
$r=1$	-	<u>-1 +2 -1 +2 -1 +2 -1</u>	0 0 -1 +2 -1 +2 -1	0 0 0 0 -1 +2 -1	0 0 0 0 0 0 -1	-	-	-	-
$r=2$	-	-	<u>0 -2 +3 -2 +3 -2 +3</u>	0 0 0 -2 +3 -2 +3	0 0 0 0 -2 3	No change	-	-	-
$r=3$	-	-	-	<u>0 0 -3 +4 -3 +4 -3</u>	0 0 0 0 -3 +4 -3	0 0 0 0 0 0 -3	-	-	-
$r=4$	-	-	-	-	<u>0 0 0 -4 +5 -4 +5</u>	0 0 0 0 -4 +5	No change	-	-
$r=5$	-	-	-	-	-	<u>0 0 0 0 -5 +6 -5</u>	0 0 0 0 0 -5	-	-
$r=6$	-	-	-	-	-	-	<u>0 0 0 0 0 -6 +7</u>	No change	-
$r=7$	-	-	-	-	-	-	-	<u>0 0 0 0 0 0 -7</u>	-
$r=8$	-	-	-	-	-	-	-	-	No change

corresponding number of excitations, therefore avoiding the modification in their topological properties (topological phase transition).

The first point at $|g| = \frac{1}{N-1}$ involves only a single degeneracy between the $M_0 = 0$ state and the single ($M_0 = 1, r = 1$) state. However, as one progresses to Read-Green points at higher $|g|$, more and more states will become pairwise degenerate at the Read-Green point. At the last one ($|g| = 1$), only a small minority of states (grayed-out cells) are not involved in a level crossing. While the analytical combinatorics would be fairly involved, one can check numerically for small values of even N that $\frac{N!}{[(N/2)!]^2}$ states would not undergo a level crossing at that point. While no Read-Green point will involve degeneracies over the whole spectrum that would define a true strong zero mode [36–38], the fraction of states not involved in the “strongest” zero mode (at $g = 1$), namely $\frac{N!}{2^N[(N/2)!]^2}$, becomes vanishingly small in the $N \rightarrow \infty$ thermodynamic limit.

For any given integrable Hamiltonian $H(g) = \sum_{i=1}^N \alpha_i R_i(g)$, accidental degeneracies between two states can actually occur at various values of g . Indeed, the energies $E_n = \sum_{i=1}^N \alpha_i r_i^n(g)$ and $E_m = \sum_{i=1}^N \alpha_i r_i^m(g)$ associated with two distinct eigenstates can easily become equal. However, the Read-Green points discussed in this work are radically different since they correspond to the regular set of points g at which two eigenstates can become degenerate for every possible integrable Hamiltonian $H(g)$ of this class.

The states involved in the (avoided) crossings at these points become such that their full set of eigenvalues $(r_1^n, r_2^n, \dots, r_N^n)$ and $(r_1^m, r_2^m, \dots, r_N^m)$ are identical. For any pair of eigenstates (of index n and m), the non-negative quantity $S_{nm}(g) = \sqrt{\sum_{i=1}^N [r_i^n(g) - r_i^m(g)]^2}$ can only become zero when both complete sets of eigenvalues coincide. By plotting this quantity for every pair of eigenstates, it is seen in Fig. 3 that these “complete degeneracies” only happen at the Read-Green points. One can also clearly see in the figure that higher-coupling Read-Green points involve more and more of these degeneracies.

While this study has, so far, only focused on the the $g < 0$ results, by symmetry, one can infer the corresponding $g > 0$ behavior. Indeed, at $g > 0$, the conserved charges (2) defining these systems are identical to those at $g < 0$ after inversion of the z -axis: $\hat{z} \rightarrow -\hat{z}$. Consequently, after exchanging up-spins

and down-spins ($\circ \leftrightarrow \bullet$), one can compute in the exact same way as (M_0, r) the equivalent (M_0^+, r^+) for any parent state, with $M_0^+ = N - M_m$. Since z has been inverted, one then finds that the sequence will begin with a gain of r_+ , followed by a loss of $r_+ + 1$ excitations with the sequence starting at the positive $g_s(M_0^+, r^+)$ Read-Green point. This is demonstrated in Fig. 4 where three states sharing the same value of r but different r^+ are plotted over the full range of positive and negative values of g .

Finally we verify that the proposed result holds for larger system sizes and, since the Read-Green points have an underlying topological nature [14,16,39–41], that the prescription holds true for arbitrary ϵ_i , i.e., different sets of XXZ integrable coupling constants. Such evidence is presented in Fig. 5, where three systems of $N = 14$ spins are compared for a given eigenstate.

As with every other state, size, or set of parameters we have numerically checked, the particular example presented here confirms the validity of our main result, not only in its capacity to predict the magnetization sequence but also in its independence of the specific set of chosen coupling constants.

With the specific structure of avoided crossings now understood, it becomes possible to try to exploit it in order to

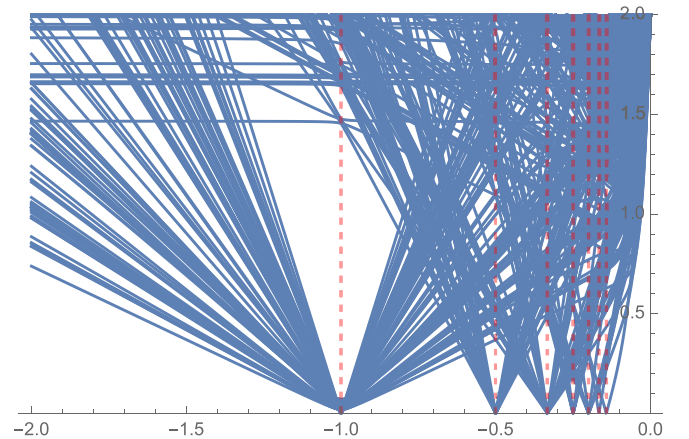


FIG. 3. “Distance” $S_{nm}(g)$ between the set of eigenvalues for every pair of eigenstates. The zeros of these functions correspond to the points where eigenstates n and m share a set of eigenvalues that are common for every conserved charge.

V. CONCLUSION

In this work, we have shown how it is possible to fully characterize the z -axis magnetization of every eigenstate of the XXZ Richardson-Gaudin models in the presence of a perturbatively weak X-Y plane magnetic field. These results also describe the number of Cooper pairs in a $p_x + ip_y$ topological superconductor weakly coupled to a particle bath. By ramping up the coupling constant g or alternatively by ramping down the z -axis magnetic field, each state undergoes a series of gain/loss of magnetization at the specific values

known as Read-Green points. We demonstrate that each of those steps, their amplitude, and the points at which they occur when ramping up g can be known in advance, for each given eigenstate, simply by knowing the spin configuration at $g = 0$, which provides the two required integers (M_0, r). These results provide a complete map of which sectors are involved in the numerous level crossings that occur in a magnetization conserving XXZ model in a z -oriented field and, equivalently, in a closed Cooper-pair-number-conserving $p + ip$ topological superconductor.

-
- [1] J. Bardeen, L. N. Cooper, and J. R. Schrieffer, *Phys. Rev.* **108**, 1175 (1957).
- [2] R. W. Richardson, *Phys. Lett.* **3**, 277 (1963).
- [3] R. W. Richardson and N. Sherman, *Nucl. Phys.* **52**, 221 (1964).
- [4] G. Sierra, J. Dukelsky, G. G. Dussel, J. von Delft, and F. Braun, *Phys. Rev. B* **61**, R11890(R) (2000).
- [5] J. von Delft and D. C. Ralph, *Phys. Rep.* **345**, 61 (2001).
- [6] D. C. Ralph, C. T. Black, and M. Tinkham, *Phys. Rev. Lett.* **74**, 3241 (1995).
- [7] C. T. Black, D. C. Ralph, and M. Tinkham, *Phys. Rev. Lett.* **76**, 688 (1996).
- [8] D. C. Ralph, C. T. Black, and M. Tinkham, *Phys. Rev. Lett.* **78**, 4087 (1997).
- [9] M. C. Cambiaggio, A. M. F. Rivas, and M. Saraceno, *Nucl. Phys. A* **624**, 157 (1997).
- [10] M. Gaudin, *J. Phys.* **37**, 1087 (1976).
- [11] M. Gaudin, *The Bethe Wavefunction* (Cambridge University Press, Cambridge, 2014).
- [12] G. Ortiz, R. Somma, J. Dukelsky, and S. Rombouts, *Nucl. Phys. B* **707**, 421 (2005).
- [13] L. Amico, A. Di Lorenzo, and A. Osterloh, *Phys. Rev. Lett.* **86**, 5759 (2001).
- [14] S. M. A. Rombouts, J. Dukelsky, and G. Ortiz, *Phys. Rev. B* **82**, 224510 (2010).
- [15] S. Lerma Hernandez, S. M. A. Rombouts, J. Dukelsky, and G. Ortiz, *Phys. Rev. B* **84**, 100503(R) (2011).
- [16] M. Ibanez, J. Links, G. Sierra, and S.-Y. Zhao, *Phys. Rev. B* **79**, 180501(R) (2009).
- [17] C. Dunning, M. Ibanez, J. Links, G. Sierra, and S.-Y. Zhao, *J. Stat. Mech.* (2010) P08025.
- [18] M. Van Raemdonck, S. De Baerdemacker, and D. Van Neck, *Phys. Rev. B* **89**, 155136 (2014).
- [19] J. Links, I. Marquette, and A. Moghaddam, *J. Phys. A* **48**, 374001 (2015).
- [20] Y. Shen, P. S. Isaac, and J. Links, *Nucl. Phys. B* **937**, 28 (2018).
- [21] N. Read and D. Green, *Phys. Rev. B* **61**, 10267 (2000).
- [22] S. Ryu, A. P. Schnyder, A. Furusaki, and A. W. W. Ludwig, *New J. Phys.* **12**, 065010 (2010).
- [23] M. Sato and Y. Ando, *Rep. Prog. Phys.* **80**, 076501 (2017).
- [24] S. Tewari, S. Das Sarma, C. Nayak, C. Zhang, and P. Zoller, *Phys. Rev. Lett.* **98**, 010506 (2007).
- [25] J. D. Sau, R. M. Lutchyn, S. Tewari, and S. Das Sarma, *Phys. Rev. Lett.* **104**, 040502 (2010).
- [26] S. Das Sarma, M. Freedman, and C. Nayak, *npj Quantum Inf.* **1**, 15001 (2015).
- [27] P. W. Claeys, S. De Baerdemacker, and D. Van Neck, *Phys. Rev. B* **93**, 220503(R) (2016).
- [28] P. W. Claeys, C. Dimo, S. De Baerdemacker, and A. Faribault, *J. Phys. A* **52**, 08LT01 (2019).
- [29] T. Skrypnyk, *Nucl. Phys. B* **941**, 225 (2019).
- [30] T. Skrypnyk, *J. Phys. A* **42**, 472004 (2009).
- [31] I. Lukyanenko, P. S. Isaac, and J. Links, *J. Phys. A* **49**, 084001 (2016).
- [32] J. Links, *Nucl. Phys. B* **916**, 117 (2017).
- [33] C. Dimo and A. Faribault, *J. Phys. A* **51**, 325202 (2018).
- [34] A. Faribault, P. Calabrese, and J.-S. Caux, *Phys. Rev. B* **81**, 174507 (2010).
- [35] A. Faribault, P. Calabrese, and J.-S. Caux, *J. Math. Phys.* **50**, 095212 (2009).
- [36] N. Moran, D. Pellegrino, J. K. Slingerland, and G. Kells, *Phys. Rev. B* **95**, 235127 (2017).
- [37] P. Fendley, *J. Phys. A* **49**, 30LT01 (2016).
- [38] J. F. Alicea and P. Fendley, *Annu. Rev. Condens. Matter Phys.* **7**, 119 (2016).
- [39] G. Ortiz, J. Dukelsky, E. Cobanera, C. Esebbag, and C. Beenakker, *Phys. Rev. Lett.* **113**, 267002 (2014).
- [40] G. Ortiz and E. Cobanera, *Ann. Phys.* **372**, 357 (2016).
- [41] M. S. Foster, M. Dzero, V. Gurarie, and E. A. Yuzbashyan, *Phys. Rev. B* **88**, 104511 (2013).